E&G Quaternary Sci. J., 66, 57–68, 2017
https://doi.org/10.5194/egqsj-66-57-2017

Open Access E&G Quaternary Science Journal

Research article

^{10}Be depth profiles in glacial sediments on the Swiss Plateau: deposition age, denudation and (pseudo-) inheritance

Lorenz Wüthrich[1,2,3], Claudio Brändli[3], Régis Braucher[4], Heinz Veit[1], Negar Haghipour[3], Carla Terrizzano[1,2,3], Marcus Christl[5], Christian Gnägi[1], and Roland Zech[1,2,3]

[1]Geographical Institute, University of Bern, 3012 Bern, Switzerland
[2]Oeschger Centre for Climate Change Research, University of Bern, 3012 Bern, Switzerland
[3]Geological Institute, ETH Zurich, 8093 Zurich, Switzerland
[4]Aix-Marseille Université, CNRS–IRD–Collège de France, UMR 34 CEREGE, Technopôle de l'Environnement Arbois–Méditerranée, BP80, 13545 Aix-en-Provence, France
[5]Laboratory of Ion Beam Physics, ETH Zurich, 8092 Zurich, Switzerland

Correspondence: Lorenz Wüthrich (loeru@live.com)

Relevant dates: Published: 20 December 2017

How to cite: Wüthrich, L., Brändli, C., Braucher, R., Veit, H., Haghipour, N., Terrizzano, C., Christl, M., Gnägi, C., and Zech, R.: Be depth profiles in glacial sediments on the Swiss Plateau: deposition age, denudation and (pseudo-) inheritance, E&G Quaternary Sci. J., 66, 57–68, https://doi.org/10.5194/egqsj-66-57-2017, 2017.

Abstract: During the Pleistocene, glaciers advanced repeatedly from the Alps onto the Swiss Plateau. Numeric age control for the last glaciation is good and thus the area is well suited to test a method which has so far not been applied to till in Switzerland. In this study, we apply in situ produced cosmogenic ^{10}Be depth profile dating to several till deposits. Three sites lie inside the assumed Last Glacial Maximum (LGM) extent of the Rhône and Aare glaciers (Bern, Deisswil, Steinhof) and two lie outside (Niederbuchsiten, St. Urban). All sites are strongly affected by denudation, and all sites have reached steady state, i.e., the ^{10}Be production is in equilibrium with radioactive decay and denudational losses. Deposition ages can therefore not be well constrained. Assuming constant denudation rates of 5 cm kyr^{-1}, total denudation on the order of 100 cm for sites within the extent of the LGM and up to tens of meters for older moraines are calculated. Denudation events, for example related to periglacial conditions during the LGM, mitigate the need to invoke such massive denudation and could help to explain high ^{10}Be concentrations at great depths, which we here dub "pseudo-inheritance". This term should be used to distinguish conceptionally from "true inheritance", i.e., high concentrations derived from the catchment.

Kurzfassung: Die Alpengletscher stiessen während des Pleistozäns wiederholt in das Schweizer Mittelland vor. Da die Vergletscherungsgeschichte des Mittellandes relativ gut untersucht ist, ist die Region gut geeignet um eine Methode zu testen, welche bisher noch nicht an Grundmoränen in der Schweiz angewandt wurde. Für die vorliegende Studie erstellten wir ^{10}Be Tiefenprofile für verschiedene Moränenstandorte im Schweizer Mittelland. Drei der Standorte liegen innerhalb der vermuteten LGM (Letztes Glaziales Maximum) Ausdehnung des Rhone und Aare Gletschers (Bern, Deisswil, Steinhof), zwei ausserhalb (Niederbuchsiten, St. Urban). Sämtliche Profile sind stark durch Denudation beeinflusst und alle Standorte, ausser Bern, sind im Gleichgewicht, das heisst die ^{10}Be Produktion entspricht dem radioaktiven Zerfall und Verlust durch Denudation. Exakte Depositionsalter können deshalb nicht bestimmt werden. Konstante Denudationsraten können auf ca. 5 cm kyr^{-1} geschätzt werden. Dies ergibt eine totale Denudation von ungefähr 100 cm für die LGM Profile und mehrere Meter bis Dekameter für die älteren Profile. Denudationsereignisse, hingegen, zum Beispiel in Zusammenhang mit periglazialen Bedingungen während des LGMs, erklären niedrige Oberflächenkonzentrationen auf alten Standorten und hohe ^{10}Be Konzentrationen in der Tiefe. In diesem Zusammenhang schlagen wir den Begriff "Pseudo Inheritance" vor, um konzeptionell von "Wahrer Inheritance" zu unterscheiden, welche der Präexposition im Einzugsgebiet geschuldet ist.

1 Introduction

In 1909, Albrecht Penck and Eduard Brückner published their famous and seminal three-volume work *Die Alpen im Eiszeitalter* (Penck and Brückner, 1909). They proposed four ice ages during the Quaternary: Würm, Riss, Mindel and Günz. Although mostly based on field work in the Bavarian and Austrian Alps, Penck and Brückner (1909) also applied their scheme to Switzerland. Apart from minor modifications (Eberl, 1930; Beck, 1933), the assumption that there were four glaciations in the Alps did not undergo big changes for decades. In the early 1980s, research based on palynology (Welten, 1982, 1988) and sedimentology (Schlüchter and Wolfarth-Meyer, 1986; Schlüchter, 1988, 1989b) led to a turnover of the four classical Quaternary ice ages. It was proposed that Alpine glaciers advanced at least 15 times onto the Swiss Plateau (Schlüchter, 2010; Preusser et al., 2011). New nomenclature was also introduced for the Swiss glaciations (Graf, 2009; Preusser et al., 2011; Keller and Krayss, 2011). Würm is now called Birrfeld Glaciation and encompasses marine isotope stages (MIS) 5d to 2, the penultimate glacial was renamed from Riss to Beringen and probably occurred during MIS 6 (Ivy-Ochs et al., 2006b; Graf et al., 2007, 2015), and the most extensive glaciation is now referred to as Möhlin Glaciation (> 300 ka; Graf, 2009; Preusser et al., 2011).

Since the 1960s Middle and Late Quaternary deposits of the Rhône and Aare glaciers (Fig. 1) have been investigated in several studies, focusing on glacial sediments and stratigraphy (Zimmermann, 1963), paleosols (Mailänder and Veit, 2001) and chronology (Ivy-Ochs et al., 2004; Preusser et al., 2007; Preusser, 2009). Although the extent of the Last Glacial Maximum (LGM) is controversial (Bitterli et al., 2011; Bläsi et al., 2015), the references cited above show that the chronology of the last glaciation in Switzerland is in general well established (Preusser et al., 2011). This makes the LGM deposits of the LGM Rhône and Aare glaciers suitable sites to test a method that has so far not been applied on till. In this study, we present one of the first applications of in situ produced ^{10}Be depth profile dating on moraines. In situ produced ^{10}Be is produced at the Earth surface by cosmic radiation, and production decreases exponentially with depth (Gosse and Phillips, 2001). Until now, depth profile dating has mainly been applied to terraces and alluvial fans (Hidy et al., 2010; Rixhon et al., 2011; Haghipour et al., 2014; Akçar et al., 2014; Delmas et al., 2015; Ruszkiczay-Rüdiger et al., 2016; Claude et al., 2017; Schaller et al., 2009). In order to determine the deposition age of a moraine, one would generally sample large, stable erratic boulders for ^{10}Be surface exposure dating (Heyman et al., 2016). However, boulders on the Swiss Plateau are often either completely destroyed or at least affected by human influence (Akçar et al., 2011). Under such circumstances, depth profile dating might be a promising alternative. Apart from dating, ^{10}Be depth profiles also allow to quantify denudation and inheritance (Braucher et al., 2009; Siame et al., 2004). Our study specifically aims to

i. evaluate the potential of ^{10}Be depth profile dating of moraines,

ii. investigate denudation rates and total denudation, and

iii. quantify inheritance.

2 Material and methods

2.1 Sampling sites and sampling

The research area is situated in the western part of the Swiss Plateau, which lies south of the Jura Mountains, which are built of marine sediments deposited in a shallow shelf ocean of Triassic to Jurassic age (Pfiffner, 2009). The Swiss Plateau is mainly built of clastic sediments deriving from erosion of the Alps during the Cenozoic, called the molasse (Pfiffner, 2009). For the present study we sampled till, which overlays the molasse deposits. The sampling sites are located on lateral moraines (Bern), on the valley floor (Deisswil) or on the top of molasse hills (Steinhof, Niederbuchsiten, St. Urban). Five sites have been selected for depth profile dating (Figs. 1–3). The youngest site considered in the present study is Bern, deposited by the Aare glacier during its retreat (Wüthrich et al., 2017a), followed by Deisswil and Steinhof. Both lie inside the LGM extent of the Rhône Glacier according to Bini et al. (2009). Additionally, we sampled two more depth profiles from till deposits, which are attributed to older glaciations. They are at least 130 kyr old (Preusser et al., 2011; Bitterli et al., 2011) and are situated near Niederbuchsiten and

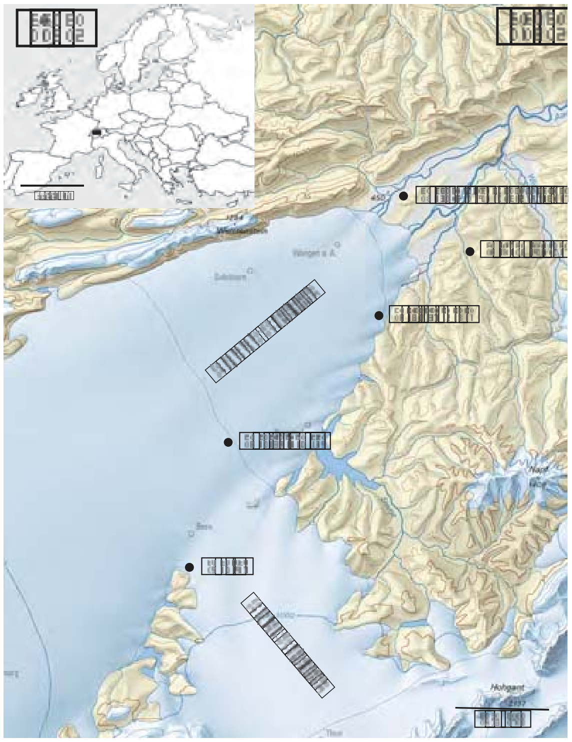

Figure 1. **(a)** Location of the research area in Europe. **(b)** LGM map of the research area modified after Bini et al. (2009). The black dots mark the sample locations (reproduced with permission of Swisstopo, BA15134). The equidistance of the contour lines is 200 m.

St. Urban. Because of the human influence on the landscape, the selection of these sites was quite challenging. As the profiles in quarry pits are already exposed, they are basically perfect for the application of depth profiles. Unfortunately, an unknown amount of material is often pushed away. In the selected quarry pits, anthropogenic removal during work in the pit was estimated based on both conversations with workers and evidence in the field. Steinhof is the only site in the present work without a quarry pit. The depth profile in this location is rather important because boulders, only several hundred meters away from the sampling site, were dated by Ivy-Ochs et al. (2004). That is why we excavated a trench using a shovel and pickaxe.

2.1.1 Bern

The profile is located in a small quarry pit right on the top of a lateral moraine, which was deposited by the Aare Glacier along the eastern slopes of Gurten mountain. According to Wüthrich et al. (2017a), the glacier retreated 18 ka from this position. The uppermost 30 cm of the sampled profile is decalcified and consists of loamy sand and some coarser clasts. Below is an unweathered, compact till, composed of clasts of diverse lithologies from the catchment of the Aare Glacier. We collected three discrete sediment samples (B1 to B3) at depths of 10, 40 and 165 cm (Table 1).

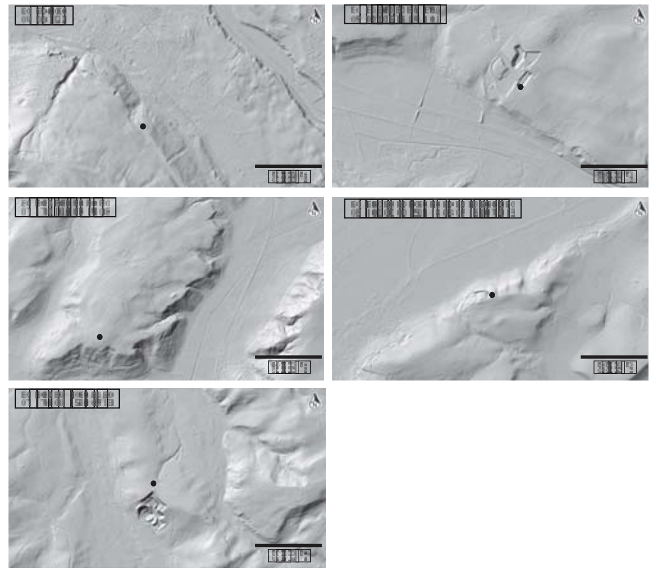

Figure 2. Digital elevation models for all sites (source: Federal Office of Topography).

2.1.2 Deisswil

Inside the extent of the LGM Rhône glacier, a gravel pit near Deisswil exposes several meters of fluvial and fluvioglacial sediments at the base and a 200 cm thick till above. The decalcification depth varies between 140 and 200 cm. Three discrete samples were collected at depths of 50, 80 and 200 cm (DW1 to 3), the lowest one being just below the local decalcification depth of 180 cm.

2.1.3 Steinhof

South of Steinhof, a 2 m deep trench was excavated close to the top of a molasse hill covered by till. According to Ivy-Ochs et al. (2004), who applied surface exposure dating on boulders at Steinhof, the Rhône Glacier reached the site during the global LGM and disappeared ∼ 24 ka. Seven discrete samples down to 190 cm were collected for the ^{10}Be depth profile (SH1 to SH7; Table 1). The sediment changes at 150 cm depth from a sandy loam with almost no pebbles, possibly a water lain till (Dreimanis, 1979), to a diamict (Flint et al., 1960a, b) with unknown thickness but at least 400 cm. The decalcification depth was reached in a drill core at 360 cm depth. The hiatus expressed in the sediments is also confirmed in the XRF data and the grain size analysis (L. Wüthrich, unpublished data).

Table 1. Locations and ^{10}Be concentrations of all samples. The steady-state denudation rate for each depth is used to find out whether the ^{10}Be concentration in the profile is in equilibrium.

Sample name	Altitude (m. a.s.l.)	Latitude (° N)	Longitude (° E)	Surface production rate (^{10}Be atoms a^{-1})	Sample depth (cm) [$g\,cm^{-2}$]	Quartz dissolved (g)	^{9}Be carrier added (mg)	^{10}Be / ^{9}Be (10^{-12})	Concentration (10^4 10Be atoms g^{-1})	Steady state denudation for ∞ time (cm kyr^{-1})
B1 (Bern)	654	46.922	7.453	7.07	10 [22]	29.3	0.3	0.118 (±0.01)	8.11 (±0.67)	6.59
B2					40 [88]	23.3	0.56	0.033 (±0.006)	2.78 (±0.48)	13.98
B3					165 [363]	8.8	0.32	0.004 (±0.002)	1.01 (±0.46)	13.76
DW1 (Deisswil)	574	47.034	7.465	6.61	50 [110]	2.8	0.31	0.076 (±0.009)	6.21 (±0.78)	5.19
DW2					80 [176]	11.7	0.42	0.08 (±0.01)	4.32 (±0.55)	5.56
DW3					200 [440]	12.7	0.3	0.017 (±0.003)	2.67 (±0.50)	3.80
SH1 (Steinhof)	593	47.155	7.682	6.71	10 [22]	42	0.3	0.16 (±0.008)	7.69 (±0.39)	6.64
SH2					30 [66]	34.2	0.3	0.109 (±0.007)	6.33 (±0.39)	6.43
SH3					60 [132]	31.1	0.38	0.043 (±0.004)	3.53 (±0.34)	8.50
SH4					90 [198]	33.3	0.3	0.045 (±0.005)	2.67 (±0.27)	8.48
SH5					120 [264]	25.1	0.3	0.026 (±0.003)	2.09 (±0.23)	8.47
SH6					150 [330]	23.8	0.3	0.03 (±0.004)	2.51 (±0.30)	5.58
SH7					190 [418]	41.7	0.31	0.034 (±0.004)	1.71 (±0.19)	6.66
NB1 (Niederbuchsiten)	483	47.286	7.77	6.13	30 [66]	44.1	0.3	0.184 (±0.009)	8.27 (±0.41)	1.57
NB2					70 [154]	10.8	0.3	0.031 (±0.004)	5.79 (±0.66)	1.72
NB3					100 [220]	38.9	0.3	0.102 (±0.007)	5.21 (±0.34)	1.58
NB4					150 [330]	47.2	0.3	0.081 (±0.008)	3.44 (±0.32)	2.10
NB5					220 [484]	46.5	0.2	0.096 (±0.007)	2.82 (±0.21)	2.20
U1 (St. Urban)	540	47.21	7.855	6.43	27.5 [60]	35.5	0.35	0.225 (±0.038)	8.79 (±1.5)	4.54
U2					66 [145]	25.3	0.25	0.155 (±0.017)	12.31 (±1.41)	2.04
U3					160 [352]	33.3	0.29	0.168 (±0.017)	9.61 (±1.08)	1.01
U4					380 [836]	51	0.51	0.170 (±0.018)	6.48 (±0.72)	0.43

2.1.4 Niederbuchsiten

The sediment located on top of a molasse hill belongs to the penultimate glaciation (Bitterli et al., 2011) and is thus at least 130 kyr old. The 10 m thick till of the Rhône glacier overlies gravel with a thickness of several decameters. We collected five samples (NB1 to NB5) for depth profile dating from 30, 70, 100, 150 and 220 cm depth (Table 1). The uppermost 20 cm of the profile consists of silty sand. This cover bed may have been deposited during the Younger Dryas (Mailänder and Veit, 2001; Semmel and Terhorst, 2010). The decalcification depth is at 300 cm.

2.1.5 St. Urban

An active quarry near St. Urban exposes freshwater molasse (Gerber and Wanner, 1984) covered by 600 cm of completely decalcified till. The deposit lies outside the extent of the LGM boundaries (Bini et al., 2009) and is thus at least 130 kyr old. We collected four samples down to a depth of 380 cm (U1 to U4; Table 1). The uppermost sample from this site comes from the ∼ 60 cm thick silty top part of the profile. The sediment was probably deposited by the ancient Rhône Glacier.

2.2 Sample preparation and AMS analyses

The depth profile samples were dispersed in Calgon and sieved to 63 to 1000 µm. We followed standard lab procedures to obtain clean quartz and then extract the beryllium (Kohl and Nishiizumi, 1992). The ^{10}Be / ^{9}Be analyses were conducted with the TANDY accelerator mass spectrometer (AMS) at the Laboratory of Ion Beam Physics, ETH Zurich. The measured ratios were normalized to the ETH Zurich in-house ^{10}Be / ^{9}Be standard S2007N with a nominal ratio of $28.10 \pm 0.76 \times 10^{-12}$ (Christl et al., 2013). Two blanks were processed together with the samples. They had ^{10}Be / ^{9}Be ratios of 0.006×10^{-12}, i.e., mostly more than 10 times smaller than the samples. The blank ratios were subtracted from the samples before calculating exposure and depth profile ages.

2.3 Depth profile calculations

Rock samples from the upper meters of Earth surface, bombarded by secondary particles originated from the cosmic rays, accumulate cosmogenic nuclide; as a result the concentration of these nuclides increase with altitude and latitude at a rate that depends on the local denudation rate. ^{10}Be is one of these in situ produced cosmogenic nuclides with a half-life of 1.387 Ma (Chmeleff et al., 2010; Korschinek et al., 2010). Its concentration reaches equilibrium as soon as the radioactive decay of ^{10}Be is equal to its production. ^{10}Be is produced by neutrogenic spallation and by muogenic interaction, mainly with oxygen (Gosse and Phillips, 2001; Heisinger et al., 2002a, b). In the last years, the application of ^{10}Be depth profiles has become an important method to date unconsolidated sediments (Hidy et al., 2010; Rixhon et al., 2011; Haghipour et al., 2014; Akçar et al., 2014; Delmas et al., 2015; Ruszkiczay-Rüdiger et al., 2016; Claude et al., 2017; Schaller et al., 2009). The advantage of this method is that it allows not only to calculate the age of the

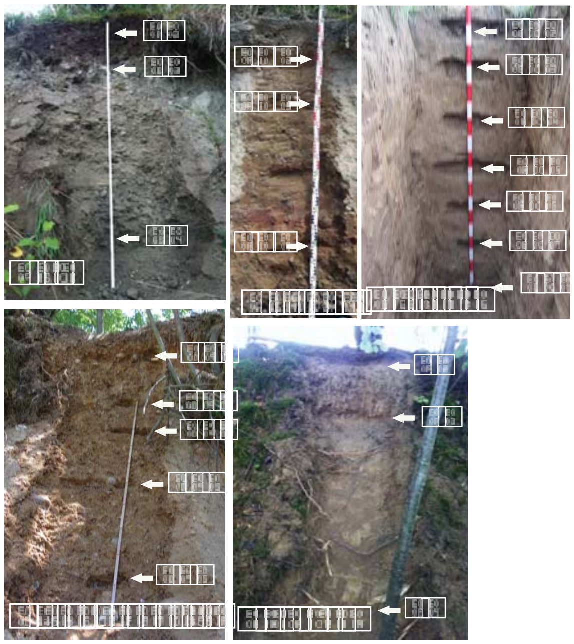

Figure 3. Photographs of the sampled profiles. U4 is not shown but is taken from the same sediment unit at 380 cm depth.

deposit but also denudation rate and the inherited share of ^{10}Be, accumulated in the catchment. As unconsolidated sediments are eroded much faster that boulders, equilibrium between production and decay is reached much faster. Because at the surface the production rate of ^{10}Be is dominated by neutrons and high, the equilibrium is reached quite quickly. Spallogenic production is exceeded by muogenic production at greater depths (Braucher et al., 2003) and it takes longer to reach steady state in deeper parts of the profile. To determine whether a depth profile has reached equilibrium, the time in Eq. (1) is set to infinity and the concentration at each depth is modeled as function of denudation rate:

$$C(z,\varepsilon,t)=\sum_i \frac{P(0)_i}{\frac{\varepsilon\cdot\rho_z}{\Lambda_i}+\lambda}\cdot e^{\left(-\frac{z\cdot\rho_z}{\Lambda_i}\right)}\cdot\left[1-e^{\left(-t\left(\frac{\varepsilon\cdot\rho_z}{\Lambda_i}+\lambda\right)\right)}\right] + C_{\mathrm{inh}}\cdot e^{-\lambda\cdot t}, \qquad (1)$$

where C is concentration (atoms g^{-1}), z is depth (cm), t is time (years), ε is denudation rate (cm a^{-1}), C_{inh} is the inherited concentration (atoms g^{-1}), $P(0)_i$ is the site-specific production rate of ^{10}Be via production pathway i, ρ_z is the cumulative bulk density (g cm^{-3}) and Λ_i is the attenuation length of pathway i (g cm^{-2}). The attenuation length is the depth in a sediment with the density ρ_z at which the production rate is $1/e$, compared to the surface production rate. When modeled steady-state denudation rates increase with depth, equilibrium has not been reached yet. Decreasing denudation rates indicate inheritance and/or complex deposition histories (Delmas et al., 2015; Ruszkiczay-Rüdiger et al., 2016). Constant denudation rates with depth indicate that the ^{10}Be production rate has reached the equilibrium and one can only calculate the minimum deposition age T_{eff} (Lal, 1991), which is the time needed to reach equilibrium with the modeled denudation rate.

$$T_{\mathrm{eff}}=\frac{1}{\lambda+\left(\frac{\rho}{\Lambda}\right)\cdot\varepsilon} \qquad (2)$$

Λ is the attenuation length of neutrons (160 g cm^{-2}).

We also used the MATLAB code version 1.2, published by Hidy et al. (2010), to calculate deposition ages, i.e., the time when the glacier has left the area, denudation rates and inheritance for our sites. The code uses a Monte Carlo approach to find solutions for Eq. (1). Apart from the measured ^{10}Be concentrations at specific depths, critical input parameters are the allowed age range (time, t), ranges for denudation rate (cm a^{-1}) and inheritance (atoms g^{-1}), as well as a denudation threshold. We used a reference production rate for neutrogenic spallation of 3.93 atoms g^{-1} a^{-1} (Heyman, 2014) and the scaling model by Lal (1991) and Stone (2000) to calculate the production rate for each site. Because the standard files for calculating muogenic production rate after Heisinger et al. (2002a, b) yield too-high values (Braucher et al., 2003, 2011, 2013; Phillips et al., 2016), we used the .m files provided Ruszkiczay-Rüdiger et al. (2016). Calculations were done until 100 000 solutions were found. No corrections were applied for snow and vegetation cover and/or shielding. For density, the allowed range was between 2.1 and 2.3 g cm^{-3}, i.e., realistic values for till (Schlüchter, 1989a).

3 Results

3.1 Bern

^{10}Be concentrations of the three samples from the Bern decrease with depth and range from 8.1×10^4 atoms g^{-1} at 10 cm depth to 1.0×10^4 atoms g^{-1} at 165 cm depth (Fig. 4, Table 1). Because of the poor fit, no reliable results could be obtained with the Hidy et al. (2010) calculator and also T_{eff} could not be calculated.

3.2 Deisswil

In the Deisswil profile, ^{10}Be concentrations decrease with depth and range from 6.2×10^4 atoms g^{-1} at 50 cm depth to 2.7×10^4 atoms g^{-1} at 200 cm depth (Fig. 4, Table 1). The steady-state denudation rate between the first and second sample does not increase with depth. Between DW2 and DW3 it does. The results from the Monte Carlo simulation did not yield any useful results and are thus not used in the paper. Minimum age T_{eff} for the uppermost two samples is 14 kyr, and calculated steady-state denudation rate is 5.2 cm kyr^{-1} (Table 2).

Table 2. Minimum ages (T_{eff}) and steady-state denudation rates for the profiles, calculated using Excel and the results of the Monte Carlo approach.

Location	Excel solutions		MATLAB solutions			
	T_{eff} (kyr)	Denudation rate (cm kyr^{-1})	Age (kyr) [2σ lower–2σ upper]	Denudation (cm kyr^{-1}) [2σ lower–2σ upper]	Inheritance (10^4 atoms g^{-1}) [2σ lower–2σ upper]	Density (g cm^{-2}) [2σ lower–2σ upper]
Deisswil	14	5.2				
Steinhof	11	6.6	16.3 [12.4–478.7]	6.2 [1.9–6.9]	0 [0–0.9]	2.278 [2.1–2.3]
Niederbuchsiten	16	4.5	21.7 [29.3–975.6]	4.9 [3.7–6.3]	2.2 [1.3–2.9]	2.138 [2.1–2.3]
St. Urban			32.6 [26.6–912.3]	2.8 [1.5–5.7]	7.3 [5.4–7.3]	2.111 [2.1–2.3]

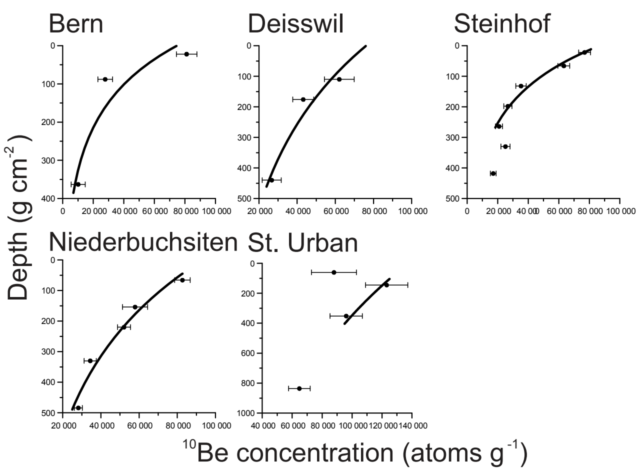

Figure 4. Measured depth profiles with error bars. The trend lines $y = a \cdot \ln(x) + b$, which calculate how the particles are attenuated are shown for the uppermost 200 cm (440 g cm^{-2}), where neutrogenic spallation is the dominant production pathway. The calculated attenuation lengths are 160 g cm^{-2} for Bern, 400 g cm^{-2} for Deisswil, 173 g cm^{-2} for Steinhof, 370 g cm^{-2} for Niederbuchsiten and 835 g cm^{-2} for St. Urban. Values exceeding 160 g cm^{-2} indicate denudational events and/or high denudation rates.

3.3 Steinhof

Concentrations decrease exponentially with depth and range from 7.7×10^4 atoms g^{-1} at 10 cm depth to 2.1×10^4 atoms g^{-1} at 120 cm depth (Fig. 4). The two lowermost samples (150 and 190 cm) have higher concentrations than expected from the exponential trend. Based on that and our sedimentological observations, we suspect that two phases of till deposition may have occurred and that the sediments below 150 cm may have experienced exposure predating the deposition of the uppermost 150 cm of the profile. The two lowermost samples were excluded from further calculations. The profile has reached steady state, with a T_{eff} of 11 kyr and a denudation rate of 6.6 cm kyr^{-1} (Table 2). The most probable Bayesian age, denudation rate and inheritance of the Monte Carlo simulation are 16.3 kyr, 6.2 cm kyr^{-1} and 0, respectively (Table 2).

3.4 Niederbuchsiten

^{10}Be concentrations in the profile near Niederbuchsiten decrease exponentially with depth and range from 8.3×10^4 atoms g^{-1} at 30 cm depth to 2.8×10^4 atoms g^{-1} at 220 cm depth (Fig. 4). The profile is in steady state with a T_{eff} and denudation rate of 16 kyr and 4.5 cm kyr^{-1} (Table 2). The Monte Carlo calculations yield 21.7 kyr, 4.9 cm kyr^{-1} and 2.2×10^4 atoms g^{-1} for age, denudation rate and inheritance, respectively (Table 2).

3.5 St. Urban

Concentrations decrease with depth and range from 12.3×10^4 atoms g^{-1} at 66 cm depth to 6.5×10^4 atoms g^{-1} at 380 cm depth (Fig. 4, Table 1). The uppermost sample from a depth of 27.5 cm has been excluded from the calculations due to its relatively low concentration of 8.8×10^4 atoms g^{-1}, which indicates that the uppermost 60 cm of the profile were deposited as loess cover long after deposition of the underlying till. The profile has reached equilibrium. In fact, steady-state denudations rates decrease with depth, indicating inheritance or a complex deposition history. We have not calculated T_{eff} because of the loess cover. The Monte Carlo calculations yield 32.6 kyr, 2.8 cm kyr^{-1} and 7.3×10^4 atoms g^{-1} for age, denudation rate and inheritance, respectively (Table 2).

4 Discussion

4.1 Ages in chronological context

The ^{10}Be concentrations in all profiles are much lower than what may be expected from the assumed deposition ages of the tills ($\sim$20 kyr and more). The uppermost samples for all profiles but St. Urban, for example, are within 10 to 50 cm from the surface but have less than 5×10^5 atoms g^{-1}. For comparison, ^{10}Be concentrations from boulder surfaces in that area with an age of $\sim$20 kyr are 2 times higher (Ivy-Ochs et al., 2004). This indicates that denudation of the landform surface has led to substantial loss of surface sediments. Ignoring denudation in the depth profile calculations would lead to an obvious, massive underestimation of the deposition ages. The low values for T_{eff} indicate that equilibrium was reached quite fast due to high denudation rates and/or denudation events.

The minimum deposition ages T_{eff} of 14, 11 and 16 kyr for Deisswil, Steinhof and Niederbuchsiten, respectively, do not provide useful age constraints and only point to high denudation. They do not even exceed the age of the Late Glacial readvances of the Gschnitz Stade in the Alps ∼ 16 ka (Ivy-Ochs et al., 2006a; Reitner, 2007; Federici et al., 2012). It is important to emphasize that the ages in this study obtained from the Monte Carlo calculations should not be overinterpreted either: The age ranges are extremely large and, more importantly, all profiles have reached equilibrium. In that sense, no meaningful age can be inferred for any site. The fact that the concentrations in the profiles have reached equilibrium is graphically also illustrated in the denudation rate–age plots (Fig. 5), where the ages go towards infinity and are only restricted by our input parameters given for the Monte Carlo approach. Solutions are found for age ranges spanning several hundreds of thousands of years, and even the 100 best fits (blue dots in Fig. 5) scatter widely and cannot provide useful constraints for the deposition ages of the moraines. However, when equilibrium is reached, denudation rates can be estimated reasonably well, and total denudation since deposition can be inferred if independent age control is available. For this purpose, we here briefly summarize the currently available data and the state of knowledge. All exposure ages have been (re)calculated using the CRONUS web calculator (Marrero et al., 2016) with the time-dependent scaling model by Lifton et al. (2014) and a reference production rate of 3.93 (±0.1) atoms g^{-1} a^{-1} (Heyman, 2014).

For the Bern site, unpublished ^{10}Be surface exposure ages on three boulders show that the Aare glacier started to retreat 18 ka from this position (Wüthrich et al., 2017a). The Deisswil site must be older than the Bern site based on stratigraphical considerations, but it is younger than Steinhof. The two oldest boulders in Steinhof (out of four) yield exposure ages of 24.4 and 23 kyr (Ivy-Ochs et al., 2004). The deposition age of the boulders in Steinhof has been questioned by Bitterli et al. (2011) and Bläsi et al. (2015) due to the high decalcification depth. At this point, we find that decalcification is also strongly affected by other factors than time – mainly the initial content of carbonates in the sediment, which decreases from west to east (Gasser and Nabholz, 1969) – and that the exposure ages are a good estimate for the deposition age of the moraine at Steinhof.

Schlüchter (1988) suggested the absence of glaciers in the Swiss Alpine Foreland during MIS 6, based on sedimentological and palynological evidence from the sections Thalgut and Meikirch, ∼ 15 km south and ∼ 10 km north of Bern, respectively.

This conflicts with the classical notion that the penultimate glaciation (i.e., Riss, Beringen, MIS 6) in the Alps was more extensive than the ultimate glaciation (Würm, Birrfeld)

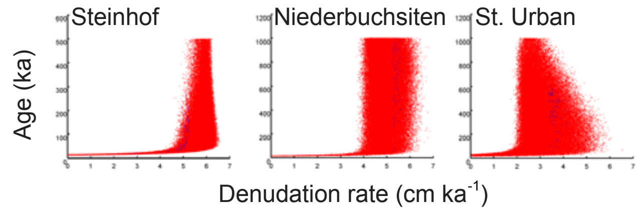

Figure 5. Denudation rate and age plots, acquired using the depth profile calculator by Hidy et al. (2010). Red dots mark all possible solutions and blue dots the 100 best χ^2 fits.

(Doppler et al., 2011; van Husen and Reitner, 2011; Preusser et al., 2011) and implies that the Niederbuchsiten till may have been deposited already during one of the early mid-Pleistocene glaciations. Attempts have been made recently to solve this controversy by applying ^{10}Be surface exposure dating on erratic boulders in the Jura Mountains by Graf et al. (2007, 2015), yet with limited success, as the oldest dated boulders date into MIS 6 but are interpreted to have been deposited much earlier. Various novel dating techniques based on luminescence and cosmogenic nuclides have been applied to sediments in Meikirch (Preusser et al., 2005) and its vicinity (Dehnert et al., 2010), and these studies do suggest that the penultimate glaciation was more extensive than the LGM. In any case, the till at Niederbuchsiten does very likely not document the oldest extensive glaciation, because it overlies fluvioglacial sediments that were deposited after an even earlier glacial advance and the respective denudational event. The till in St. Urban is completely weathered down to its base (∼ 4 m) and lies directly on molasse sediments. We can tentatively infer that it is at least MIS 6 in age and likely corresponds to the Möhlin glaciation.

4.2 Denudation rate and total denudation

The results from the Bern site do not allow to calculate age and denudation rate because of the very poor fit between the samples and the trend line (Fig. 4). We speculate that decalcification is responsible for this: decalcification means a loss of material and thus a decrease in thickness and a lowering of the surface. The samples in ^{10}Be depth profile "move" closer together. The other profiles may have been influenced by this process as well but to a lower degree, because the initial calcite content is highest in the sediments of the Aare Glacier and decreases from west to east in the deposits of the Rhône Glacier (Gasser and Nabholz, 1969). Decalcification cannot yet be corrected for and will be ignored in the following discussion.

The steady-state denudation rates of 5.2 and 6.6 cm kyr^{-1} for Deisswil and Steinhof are comparable to the most probable Bayesian denudation rates of 6.2 cm kyr^{-1} for Steinhof. Assuming constant denudation rates of ∼ 6 cm kyr^{-1} and exposure ages of ∼ 24 kyr for these three sites yields total denudation on the order of 120 cm. Denudation was probably not constant over time, and another back-of-the-envelope calculation could assume most recent denudation due to anthropogenic activity. As the ^{10}Be production decreases to half of its surface value at ∼ 50 cm depth, total denudation would thus be at least on that order of magnitude.

For the Niederbuchsiten site denudation rates between 3.7 and 6.3 cm kyr^{-1} can be modeled (Table 2), yet all best fits are close to the most probable Bayesian denudation rate of 4.9 cm kyr^{-1} and the steady-state denudation of 4.5 cm kyr^{-1} (Fig. 5). Assuming constant denudation on that order of magnitude yields a total denudation of > 6 m in the case that the till was deposited during the Beringen Glaciation (MIS 6). In the case that the till at Niederbuchsiten was deposited during MIS 8, 300 ka or earlier, a total denudation of > 13 m can be calculated. Again, however, constant denudation is unlikely, particularly in view of the old age spanning at least one glacial–interglacial cycle, and we evaluate an alternative more complex scenario: as the ^{10}Be production decreases to 10 % of its surface value at ∼ 380 g cm^{-2} (∼ 170 cm with a density of 2.2 g cm^{-2}) depth, deposition during MIS 6 and the most recent anthropogenic truncation of the profile on that order of magnitude is one scenario. Also, periglacial solifluction during the LGM may have removed much of the ^{10}Be that accumulated close to the surface since MIS 6. In that case denudation must additionally have been active since the LGM because, like in the case of Steinhof, Deisswil and Bern, the surface ^{10}Be concentration at Niederbuchsiten is only about half of the concentration than one would expect from a stable surface exposed since the LGM.

The denudation rates obtained from the Monte Carlo simulations for St. Urban are between 1.5 and 5.7 cm kyr^{-1} and the most probable Bayesian denudation rate is 2.8 cm kyr^{-1} (Table 2, Fig. 5c). With such denudation rates, one would calculate ∼ 4 m total denudation if the till was deposited during the penultimate glaciation and ∼ 25 m if the till was deposited 800 ka. Again, several meters of denudation due to intensive periglacial dynamics during the LGM (and possibly earlier) could have played an important role in lowering the ^{10}Be concentrations. For St. Urban, this is most probably the case, because the depth profile can be fitted best with an attenuation length of 835 g cm^{-2} (Fig. 4). Such a high value strongly exceeds the attenuation length of 160 g cm^{-2} related to neutrogenic production (dominant only near the surface) and points to a significant muogenic contribution (1500 g cm^{-2} for slow muons and 4320 g cm^{-2} for fast muons; Braucher et al., 2009, 2013). The attenuation lengths are expressed in the slope (a) of the trend line in Fig. 4. Interestingly, Niederbuchsiten also shows this indication for massive denudation (fitted attenuation lengths of 370 g cm^{-2}), although not to such a degree, whereas Bern and Steinhof do not, consistent with their presumably last glacial age.

We conclude that denudation rates can be reasonably constrained with the help of ^{10}Be depth profiles, and total denudation can be estimated provided that the deposition age of the parent material is known. This works particularly well for sites not older than the LGM, where constant denudation rates are ∼ 5 cm kyr^{-1} and total denudation is on the order of 0.5 to 1 m. For older sites, constant denudation rates can be constrained by the Monte Carlo simulations to 3–5 cm kyr^{-1}. However, the assumption of constant denudation is very likely wrong and would result in several meters of total denudation for MIS 6 sites and even several tens of meters for older sites. Total denudation of even more than 100 m is necessary to explain the ^{10}Be depth profiles in Deckenschotter (Häuselmann et al., 2007; Akçar et al., 2014; Claude et al., 2017). We suggest that denudational events related to periglacial dynamics might play an important role for the denudation history. This would substantially mitigate the need to invoke massive total denudation. It might therefore be a promising endeavor for future studies to modify the Monte Carlo simulations in a way that denudational events can be evaluated.

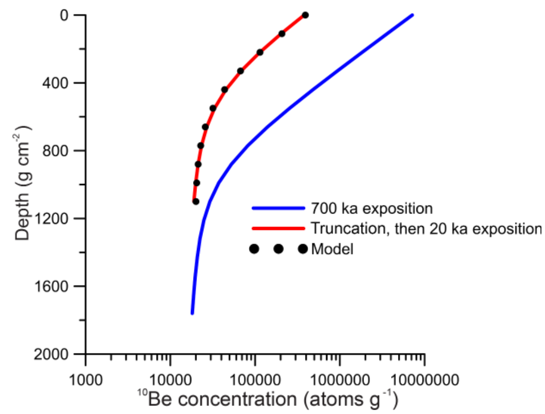

Figure 6. Illustration of "pseudo-inheritance". The plot shows a theoretical profile which was exposed for 700 kyr. Then 3 m were truncated immediately. Afterwards, the profile was again exposed to the cosmic radiation for 20 kyr. We modeled the age (31 kyr) and inheritance (19 × 10^4 atoms g^{-1}) using excel.

4.3 Inheritance and "pseudo-inheritance"

The most probable Bayesian inheritance is zero for Steinhof (Table 2) and also low for Bern and Deisswil (Fig. 4), whereas Niederbuchsiten and St. Urban have a much higher inheritance of 2.2 × 10^4 and 7.3 × 10^4 atoms g^{-1} (Table 2). This might be a systematic pattern, with less inheritance for the younger sites and more inheritance for the older ones. The pattern might document that the earlier glacial advances eroded a landscape that had accumulated substantial amounts of cosmogenic nuclides near the surface before the onset of the massive glaciations. During the course of the Pleistocene glaciations, the glaciers eroded deeper and deeper and therefore transported and deposited sediments with less inheritance. In the following, however, we elucidate that the high inheritance in Niederbuchsiten and St. Urban may not necessarily reflect "true" inheritance from the catchment but can alternatively be explained with denudation events during the long exposure history of the sites since deposition.

When a site is exposed to cosmic radiation over hundreds of thousands of years, notable amounts of ^{10}Be are produced not only at the surface but also at greater depth, mostly due to muogenic production (Heisinger et al., 2002a, b; Braucher et al., 2003, 2011, 2013). Massive denudation, related for example to periglacial conditions, could truncate the site but still leave considerable amounts of these muogenic ^{10}Be atoms that decrease in concentration with depth with a much smaller slope than ^{10}Be atoms that are produced close to the surface by neutrons. New exposure after the denudational event leads to accumulation of new ^{10}Be, and the concentration in the upper few meters will soon again have the steep slope related to the neutron flux. When age, constant denudation and inheritance are calculated from such a depth profile, the high ^{10}Be concentration at depth is therefore wrongly interpreted as inheritance. We dub the high concentration at depth "pseudo-inheritance" when it is the result of long exposure of the site and massive denudation rather than "true" inheritance from the catchment.

To illustrate the concept of pseudo-inheritance, we create a 800 cm deep depth profile that has experienced a 700 kyr long exposition without denudation. Then we truncate 300 cm in a single event. After that, we allow an exposure of 20 kyr without denudation. In the following, we modeled the concentrations using Excel with unconstrained inheritance and age and zero denudation (Fig. 6). The results yield a best fit age of 31 kyr and an inheritance of 19×10^4 atoms g^{-1}. The young apparent age and high apparent inheritance reflect the denudational loss of the neutron component and the dominance of the muogenic component, respectively. The apparent inheritance is *not* derived from the catchment and should not be confused with "true" inheritance.

5 Conclusions

- Our results show that ^{10}Be depth profiles on the Swiss Plateau reach steady state within a few thousand years and do not provide new robust age control for the timing of Pleistocene glaciation.
- Concentrations of the Niederbuchsiten and St. Urban profiles decrease with a suspiciously low slope, possibly indicating significant muogenic contributions, pre-LGM deposition ages and massive denudation since deposition.
- The ^{10}Be depth profiles can be used to reasonably constrain modeled constant denudation rates to ~ 5 cm kyr^{-1}. Given independent age constraints for the MIS 2 sites, total denudation amounted to ~ 100 cm since deposition. Alternatively, most recent anthropogenic denudation would be on the order of 50 cm to explain the low ^{10}Be concentrations at all three sites.
- For Niederbuchsiten and St. Urban, the ^{10}Be depth profiles also yield denudation rates of ~ 5 cm kyr^{-1}, but the assumption of constant denudation would imply several or even tens of meters of total denudation. Denudation events related to periglacial activity, for example during the LGM, would substantially mitigate the need to invoke massive total denudation. Only a few meters of periglacial denudation during glaciations would be sufficient to explain the low observed ^{10}Be concentrations. Massive denudation and/or denudation events result in relatively high concentrations at depth stemming from muogenic production, and as this may wrongly be interpreted as inheritance, we dub this phenomenon "pseudo-inheritance". Modifications in the depth profile calculations should be made so that denudation events can be included in the Monte Carlo simulations.

We finally conclude that ^{10}Be depth profiles are an innovative tool to quantitatively investigate Earth surface processes. Deposition ages can be inferred for fluvial terraces and moraines, yet ages should always be discussed in context with denudation, which itself is generally poorly constrained. We see great potential for studying denudation histories at specific sites and for whole catchments, where the age of the parent material is known independently. In the future, dating of soft sediments in such a dynamic environment as the Swiss Plateau with high denudation rates can be improved with the combination of samples from shallow depths, with many more samples (than in this study) from greater depths (> 700 g cm^{-2}), which allows us to calculate denudation in steady state from the upper part and better constrained ages from the lower part. Also the combination of several cosmogenic nuclides might help to (i) constrain the timing of denudational events in the past (Fülöp et al., 2015) and (ii) obtain burial ages (Balco and Rovey, 2008).

Data availability. The dataset used in this paper can be found on the Pangaea database (Wüthrich et al., 2017b).

Competing interests. The authors declare that they have no conflict of interest.

Acknowledgements. We thank the SNSF for funding (PZ00P2_131670, PP00P2 150590). Marcel Bliedtner, Zsófia Ruszkiczay-Rüdiger, Imke Schäfer and Mareike Trauerstein are thanked for proof reading and fruitful discussions. Gilles Rixhon and an anonymous reviewer are thanked for their reviews.

References

Akçar, N., Ivy-Ochs, S., Kubik, P. W., and Schlüchter, C.: Post-depositional impacts on "Findlinge" (erratic boulders) and their implications for surface-exposure dating, Swiss J. Geosci., 104, 445–453, https://doi.org/10.1007/s00015-011-0088-7, 2011.

Akçar, N., Ivy-Ochs, S., Alfimov, V., Claude, A., Graf, H. R., Dehnert, A., Kubik, P. W., Rahn, M., Kuhlemann, J., and Schlüchter, C.: The first major incision of the Swiss Deckenschotter landscape, Swiss J. Geosci., 107, 337–347, https://doi.org/10.1007/s00015-014-0176-6, 2014.

Balco, G. and Rovey, C. W.: A isochron method for cosmogenic-nuclide dating of buried soils and sediments, Am. J. Sci., 308, 1083–1114, https://doi.org/10.2475/10.2008.02, 2008.

Beck, P.: Über das schweizerische und europäische. Pliozän und Pleistozän, Eclogae Geol. Helv., 26, 335–437, 1933.

Bini, A., Buonchristiani, J.-F., Couterand, S., Ellwanger D., Felber, M., Florineth, D., Graf, H. R., Keller, O., Kelly, M., Schlüchter, C., and Schöneich, P.: Die Schweiz während des letzteiszeitlichen Maximums (LGM), Bundesamt für Landestopografie, Wabern, 2009.

Bitterli, T., Jordi, H., Gerber, M., Gnaegi, C., and Graf, H. R.: Geologischer Atlas der Schweiz: Blatt 1108: Murgenthal (Erlaeuterungen), Bundesamt für Landestopografie, Wabern, 2011.

Bläsi, H. R., Gygi, R., Gnägi, C., Graf, H. R., Jordan, P., Labscher, H. P., Ledermann, H., Herold, T., Schlanke, S., Burkhalter, R., and Kälin, D.: Geologischer Atlas der Schweiz. Blatt 1107: Balsthal (Erlaeuterungen), Bundesamt für Landestopografie, Wabern, Switzerland, 2015.

Braucher, R., Brown, E. T., Bourlès, D. L., and Colin, F.: In situ produced ^{10}Be measurements at great depths: implications for production rates by fast muons, Earth Planet. Sc. Lett., 211, 251–258, 2003.

Braucher, R., Del Castillo, P., Siame, L., Hidy, A. J., and Bourles, D. L.: Determination of both exposure time and denudation rate from an in situ-produced ^{10}Be depth profile: a mathematical proof of uniqueness. Model sensitivity and applications to natural cases, Quat. Geochronol., 4, 56–67, 2009.

Braucher, R., Merchel, S., Borgomano, J., and Bourlès, D. L.: Production of cosmogenic radionuclides at great depth: a multi element approach, Earth Planet. Sc. Lett., 309, 1–9, 2011.

Braucher, R., Bourlès, D., Merchel, S., Vidal Romani, J., Fernadez-Mosquera, D., Marti, K., Léanni, L., Chauvet, F., Arnold, M., Aumaître, G., and Keddadouche, K.: Determination of muon attenuation lengths in depth profiles from in situ produced cosmogenic nuclides, Nucl. Instrum. Meth. B, 294, 484–490, https://doi.org/10.1016/j.nimb.2012.05.023, 2013.

Chmeleff, J., von Blanckenburg, F., Kossert, K., and Jakob, D.: Determination of the ^{10}Be half-life by multicollector ICP-MS and liquid scintillation counting, Nucl. Instrum. Meth. B, 268, 192–199, 2010.

Christl, M., Vockenhuber, C., Kubik, P. W., Wacker, L., Lachner, J., Alfimov, V., and Synal, H.-A.: The ETH Zurich AMS facilities. Performance parameters and reference materials, Nucl. Instrum. Meth. B, 294, 29–38, https://doi.org/10.1016/j.nimb.2012.03.004, 2013.

Claude, A., Akçar, N., Ivy-Ochs, S., Schlunegger, F., Kubik, P. W., Dehnert, A., Kuhlemann, J., Rahn, M., and Schlüchter, C.: Timing of early Quaternary gravel accumulation in the Swiss Alpine Foreland, Geomorphology, 276, 71–85, https://doi.org/10.1016/j.geomorph.2016.10.016, 2017.

Dehnert, A., Preusser, F., Kramers, J. D., Akcar, N., Kubik, P. W., Reber, R., and Schlüchter, C.: A multi-dating approach applied to proglacial sediments attributed to the Most Extensive Glaciation of the Swiss Alps, Boreas, 39, 620–632, 2010.

Delmas, M., Braucher, R., Gunnell, Y., Guillou, V., Calvet, M., Bourlès, D., and ASTER Team: Constraints on Pleistocene glaciofluvial terrace age and related soil chronosequence features from vertical ^{10}Be profiles in the Ariege River catchment (Pyrenees, France), Global Planet. Change, 132, 39–53, 2015.

Doppler, G., Krömer, E., Rögner, K., Wallner, J., Jerz, H., Grottenthaler, W.: Quaternary Stratigraphy of Southern Bavaria, Quaternary Science Journal, 60, 329–365, https://doi.org/10.3285/eg.60.2-3.08, 2011.

Dreimanis, A.: The problem of waterlain tills, in: Moraines and varves, edited by: Schlüchter, C., A.A. Balkema, Rotterdam, the Netherlands, 167–175, 1979.

Eberl, B.: Die Eiszeitfolge im nürdlichen Alpenvorland, ihr Ablauf, ihre Chronologie auf Grund der Aufnahme im Bereich des Lech- und Illergletschers, Benno Filzer, Augsburg, Germany, 1930.

Federici, P. R., Granger, D. E., Ribolini, A., Spagnolo, M., Pappalardo, M., and Cyr, A. J.: Last Glacial Maximum and the Gschnitz stadial in the Maritime Alps according to ^{10}Be cosmogenic dating, Boreas, 41, 277–291, https://doi.org/10.1111/j.1502-3885.2011.00233.x, 2012.

Flint, R. F., Sanders, J. E., and Rodgers, J.: Diamictite: A substitute term for Symmictite, Geol. Soc. Am. Bull., 71, 1809–1810, 1960a.

Flint, R. F., Sanders, J. E., and Rodgers, J.: Symmictite: A name for nonsorted terrigenous sedimentary rocks that contain a wide range of particle sizes, Geol. Soc. Am. Bull., 71, 507–510, 1960b.

Fülöp, R.-H., Bishop, P., Fabel, D., Cook, G. T., Everest, J., Schnabel, C., Codilean, A. T., and Xu, S.: Quantifying soil loss with in situ ^{10}Be and ^{14}C depth-profiles, Quat. Geochronol., 27, 78–93, 2015.

Gasser, U. and Nabholz, W.: Zur Sedimentologie der Sandfraktion im Pleistozän des schweizerischen Mittellander, Eclogae Geol. Helv., 62, 467–516, 1969.

Gerber, M. E. and Wanner, J.: Blatt 1128: Langenthal, Schweizerische Geologische Kommission (Geologischen Atlas der Schweiz 1 : 25 000), 1984.

Gosse, J. C. and Phillips, F. M.: Terrestrial in situ cosmogenic nuclides: theory and application, Quaternary Sci. Rev., 20, 1475–1560, https://doi.org/10.1016/S0277-3791(00)00171-2, 2001.

Graf, H. R.: Stratigraphie von Mittel- und Spätpleistozän in der Nordschweiz, Beiträge zur Geologischen Karte der Schweiz 168, Bundesamt für Landestopografie swisstopo, Wabern, 2009.

Graf, A. A., Strasky, S., Ivy-Ochs, S., Akcar, N., Kubik, P. W., Burkhard, M., and Schlüchter, C.: First results of cosmogenic dated pre-Last Glaciation erratics from the Montoz area, Jura Mountains, Switzerland, Quaternary Int., 164165, 43–52, https://doi.org/10.1016/j.quaint.2006.12.022, 2007.

Graf, A. A., Akçar, N., Ivy-Ochs, S., Strasky, S., Kubik, P. W., Christl, M., Burkhard, M., Wieler, R., and Schlüchter, C.: Multiple advances of Alpine glaciers into the Jura Mountains in the Northwestern Switzerland, Swiss J. Geosci., 108, 225–238, https://doi.org/10.1007/s00015-015-0195-y, 2015.

Haghipour, N., Burg, J.-P., Ivy-Ochs, S., Hajdas, I., Kubik, P., and Christl, M.: Correlation of fluvial terraces and temporal steady-state incision on the onshore Makran accretionary wedge in southeastern Iran: Insight from channel profiles and ^{10}Be exposure dating of strath terraces, Geol. Soc. Am. Bull., 127, 560–583, https://doi.org/10.1130/B31048.1, 2014.

Häuselmann, P., Fiebig, M., Kubik, P. W., and Adrian, H.: A first attempt to date the original "Deckenschotter" of Penck and Brückner with cosmogenic nuclides, From the Swiss Alps to the Crimean Mountains – Alpine Quaternary stratigraphy in a European context, 164–165, 33–42, https://doi.org/10.1016/j.quaint.2006.12.013, 2007.

Heisinger, B., Lal, D., Jull, A. T., Kubik, P., Ivy-Ochs, S., Knie, K., and Nolte, E.: Production of selected cosmogenic radionuclides by muons: 2. Capture of negative muons, Earth Planet. Sc. Lett., 200, 357–369, 2002a.

Heisinger, B., Lal, D., Jull, A. T., Kubik, P., Ivy-Ochs, S., Neumaier, S., Knie, K., Lazarev, V., and Nolte, E.: Production of selected cosmogenic radionuclides by muons: 1. Fast muons, Earth Planet. Sc. Lett., 200, 345–355, 2002b.

Heyman, J.: Paleoglaciation of the Tibetan Plateau and surrounding mountains based on exposure ages and ELA depression estimates, Quaternary Sci. Rev., 91, 30–41, https://doi.org/10.1016/j.quascirev.2014.03.018, 2014.

Heyman, J., Applegate, P. J., Blomdin, R., Gribenski, N., Harbor, J. M., and Stroeven, A. P.: Boulder height – exposure age relationships from a global glacial ^{10}Be compilation, Quat. Geochronol., 34, 1–11, https://doi.org/10.1016/j.quageo.2016.03.002, 2016.

Hidy, A. J., Gosse, J. C., Pederson, J. L., Mattern, J. P., and Finkel, R. C.: A geologically constrained Monte Carlo approach to modeling exposure ages from profiles of cosmogenic nuclides: An example from Lees Ferry, Arizona, Geochem. Geophy. Geosy., 11, Q0AA10, https://doi.org/10.1029/2010GC003084, 2010.

Ivy-Ochs, S., Schäfer, J., Kubik, P. W., Synal, H.-A., Schlüchter, C.: Timing of deglaciation on the northern Alpine foreland (Switzerland), Eclogae Geol. Helv., 97, 47–55, https://doi.org/10.1007/s00015-004-1110-0, 2004.

Ivy-Ochs, S., Kerschner, H., Kubik, P. W., and Schlüchter, C.: Glacier response in the European Alps to Heinrich Event 1 cooling: the Gschnitz stadial, J. Quaternary Sci., 21, 115–130, 2006a.

Ivy-Ochs, S., Kerschner, H., Reuther, A., Maisch, M., Sailer, R., Schäfer, J., Kubik, P. W., Synal, H.-A., and Schlüchter, C.: The timing of glacier advances in the northern European Alps based on surface exposure dating with cosmogenic ^{10}Be, ^{26}Al, ^{36}Cl, and ^{21}Ne, Geol. S. Am. S., 415, 43–60, https://doi.org/10.1130/2006.2415(04), 2006b.

Keller, O. and Krayss, E.: Mittel- und spätpleistozäne Stratigraphie und Morphogenese in Schlüsselregionen der Nordschweiz, E&G Quaternary Sci. J., 59, 88–119, https://doi.org/10.3285/eg.59.1-2.08, 2011.

Kohl, C. and Nishiizumi, K.: Chemical isolation of quartz for measurement of in-situ -produced cosmogenic nuclides, Geochim. Cosmochim. Ac., 56, 3583–3587, https://doi.org/10.1016/0016-7037(92)90401-4, 1992.

Korschinek, G., Bergmaier, A., Faestermann, T., Gerstmann, U. C., Knie, K., Rugel, G., Wallner, A., Dillmann, I., Dollinger, G., Gostomski, C. L. von, Kossert, K., Maiti, M., Poutivtsev, M., and Remmert, A.: A new value for the half-life of ^{10}Be by Heavy-Ion Elastic Recoil Detection and liquid scintillation counting, Nucl. Instrum. Meth. B, 268, 187–191, https://doi.org/10.1016/j.nimb.2009.09.020, 2010.

Lal, D.: Cosmic ray labeling of erosion surfaces: in situ nuclide production rates and erosion models, Earth Planet. Sc. Lett., 104, 424–439, https://doi.org/10.1016/0012-821X(91)90220-C, 1991.

Lifton, N., Sato, T., and Dunai, T. J.: Scaling in situ cosmogenic nuclide production rates using analytical approximations to atmospheric cosmic-ray fluxes, Earth Planet. Sc. Lett., 386, 149–160, https://doi.org/10.1016/j.epsl.2013.10.052, 2014.

Mailänder, R. and Veit, H.: Periglacial cover- beds on the Swiss Plateau: Indicatords of soil, climate and landscape evolution during the Late Quaternary, CATENA, 45, 251–272, https://doi.org/10.1016/S0341-8162(01)00151-5, 2001.

Marrero, S. M., Phillips, F. M., Borchers, B., Lifton, N., Aumer, R., and Balco, G.: Cosmogenic nuclide systematics and the CRONUScalc program, Quat. Geochronol., 31, 160–187, https://doi.org/10.1016/j.quageo.2015.09.005, 2016.

Penck, A. and Brückner, E.: Die Alpen im Eiszeitalter, 3 Vol., C. H. Tauchnitz, Leipzig, Germany, 1909.

Pfiffner, O. A.: Geologie der Alpen, 1st Edn., Haupt (UTB, 8416), Bern, 2009.

Phillips, F. M., Argento, D. C., Balco, G., Caffee, M. W., Clem, J., Dunai, T. J., Finkel, R., Goehring, B., Gosse, J. C., Hudson, A. M., Jull, A. T., Kelly, M. A., Kurz, M., Lal, D., Lifton, N., Marrero, S. M., Nishiizumi, K., Reedy, R. C., Schaefer, J., Stone, J. O., Swanson, T., and Zreda, M. G.: The CRONUS-Earth Project: A synthesis, Quat. Geochronol., 31, 119–154, https://doi.org/10.1016/j.quageo.2015.09.006, 2016.

Preusser, F.: Towards a chronology of the late Pleistocene in the northern Alpine Foreland, Boreas, 33, 195–210, https://doi.org/10.1111/j.1502-3885.2004.tb01141.x, 2009.

Preusser, F., Drescher-Schneider, R., Fiebig, M., and Schlüchter, C.: Re-interpretation of the Meikirch pollen record, Swiss Alpine Foreland, and implications for Middle Pleistocene chronostratigraphy, J. Quaternary Sci., 20, 607–620, https://doi.org/10.1002/jqs.930, 2005.

Preusser, F., Blei, A., Graf, H., and Schlüchter, C.: Luminescence dating of Würmian (Weichselian) proglacial sediments from Switzerland: methodological aspects and stratigraphical conclusions, Boreas, 36, 130–142, https://doi.org/10.1111/j.1502-3885.2007.tb01187.x, 2007.

Preusser, F., Graf, H. R., Keller, O., Krayss, E., and Schlüchter, C.: Quaternary glaciation history of northern Switzerland, E&G Quaternary Sci. J., 60, 282–305, 2011.

Reitner, J. M.: Glacial dynamics at the beginning of Termination I in the Eastern Alps and their stratigraphic implications, Quaternary Int., 164, 64–84, 2007.

Rixhon, G., Braucher, R., Bourlès, D., Siame, L., Bovy, B., and Demoulin, A.: Quaternary river incision in NE Ardennes (Belgium) – Insights from ^{10}Be/^{26}Al dating of river terraces, Quat. Geochrono., 6, 273–284, https://doi.org/10.1016/j.quageo.2010.11.001, 2011.

Ruszkiczay-Rüdiger, Z., Braucher, R., Novothny, Á., Csillag, G., Fodor, L., Molnár, G., Madarász, B., and ASTER Team: Tectonic and climatic control on terrace formation: Coupling in situ produced ^{10}Be depth profiles and luminescence approach, Danube River, Hungary, Central Europe, Quaternary Sci. Rev., 131, 127–147, 2016.

Schaller, M., Ehlers, T. A., Blüm, J. D., and Kallenberg, M. A.: Quantifying glacial moraine age, denudation and soil mixing with cosmogenic nuclide depth profiles, J. Geophys. Res., 114, F01012, https://doi.org/10.1029/2007JF000921, 2009.

Schlüchter, C.: A non-classical summary of the Quaternary stratigraphy in the northern Alpine foreland of Switzerland, Bulletin de la Société neuchâteloise de géographie, 23, 143–157, 1988.

Schlüchter, C.: Eiszeitliche Lockergesteine- Geologie, Genese und Eigenschaften. Ein Beitrag zu den Beziehungen zwischen fundamentaler und angewandter Eiszeitgeologie, Habilitationsschrift, ETH Zürich, 1989a.

Schlüchter, C.: The most complete quaternary record of the Swiss Alpine Foreland, Palaeogeogr. Palaeocl., 72, 141–146, https://doi.org/10.1016/0031-0182(89)90138-7, 1989b.

Schlüchter, C.: Das Eiszeitalter der Schweiz-. Eine schematische Zusammenfassung, Institut für Geologie der Universität Bern, 2010.

Schlüchter, C. and Wolfarth-Meyer, B.: Till facies varieties of the Western Swiss Alpine Foreland, in: Till and Glaciotectonics, edited by: van der Meer, J. J. M., A.A. Balkema, Rotterdam, the Netherlands, 67–72, 1986.

Semmel, A. and Terhorst, B.: The concept of the Pleistocene periglacial cover beds in central Europe: a review, Quaternary Int., 222, 120–128, 2010.

Siame, L., Bellier, O., Braucher, R., Sébrier, M., Cushing, M., Bourlès, D., Hamelin, B., Baroux, E., de Voogd, B., Raisbeck, G., and Yiou, F.: Local erosion rates versus active tectonics: cosmic ray exposure modelling in Provence (south-east France), Earth Planet. Sc. Lett., 220, 345–364, 2004.

Stone, J. O.: Air pressure and cosmogenic isotope production, J. Geophys. Res.-Sol. Ea., 105, 23753–23759, https://doi.org/10.1029/2000JB900181, 2000.

van Husen, D. and Reitner, J. M.: An outline of the Quaternary stratigraphy of Austria, Eiszeitalter und Gegenwart, 60, 366–387, 2011.

Welten, M.: Pollenanalytische Untersuchungen im jüngeren Quartär des nördlichen Alpenvorlandes der Schweiz, Stämpfli (Beiträge zur geologischen Karte der Schweiz, 156), Bern, 1982.

Welten, M.: Neue pollenanalytische Ergebnisse über das Jüngere Quartär des nördlichen Alpenvorlandes der Schweiz (Mittel- und Jungpleistozän), Stämpfli (Beiträge zur geologischen Karte der Schweiz, 162), Bern, 1988.

Wüthrich, L., Garcia Morabito, E., Zech, J., Gnägi, C., Trauerstein, M., Veit, H., Merchel, S., Scharf, A., Rugel, G., Christl, M., and Zech, R.: ^{10}Be surface exposure dating of the last deglaciation in the Aare Valley, Switzerland, Swiss J. Geosci., submitted, 2017a.

Wüthrich, L., Brändli, C., Braucher, R., Veit, H., Haghipour, N., Terrizzano, C., Christl, M., Gnägi, C., and Zech, R.: Beryllium 10 (^{10}Be) concentrations from till in the western Swiss lowlands, PANGAEA, https://doi.org/10.1594/PANGAEA.884060, 2017b.

Zimmermann, H. W.: Die Eiszeit im westlichen zentralen Mittelland (Schweiz), Separat Abdruck aus den Mitteilungen der Naturforschenden Gesellschaft Solothurn, 21, 10–143, 1963.